Use of contact testing in the characterization and design of all-ceramic crownlike layer structures: A review

Brian R. Lawn, BSc, PhD,[a] Yan Deng, BEng,[b] and Van P. Thompson, DDS, PhD[c]
National Institute of Standards and Technology, Gaithersburg, Md.; University of Maryland, College Park, Md.; and University of Medicine and Dentistry at New Jersey, Newark, N.J.

Ceramic-based crowns, particularly molar crowns, can fail prematurely from accumulation of fracture and other damage in continual occlusal contact. Damage modes depend on ceramic types (especially microstructures), flaw states, loading conditions, and geometric factors. These damage modes can be simulated and characterized in the laboratory with the use of Hertzian contact testing on monolayer, bilayer, and trilayer structures to represent important aspects of crown response in oral function. This article reviews the current dental materials knowledge base of clinically relevant contact-induced damage in ceramic-based layer structures in the context of all-ceramic crown lifetimes. It is proposed that simple contact testing protocols that make use of sphere indenters on model flat, ceramic-based layer structures—ceramic/polymer bilayers (simulating monolithic ceramic crowns on dentin) and ceramic/ceramic/polymer trilayers (simulating veneer/core all-ceramic crowns on dentin)—can provide useful relations for predicting critical occlusal loads to induce lifetime-threatening fracture. It is demonstrated that radial cracking from the lower core layer surface is the dominant failure mode for ceramic layer thicknesses much below 1 mm. Such an approach may be used to establish a scientific, materials-based foundation for designing next-generation crown layer structures. (J Prosthet Dent 2001;86:495-510.)

Ceramics are attractive dental crown materials because of their superior aesthetics, inertness, and biocompatibility. However, ceramics are brittle and subject to premature failure, especially in repeated contact loading and moist environments.[1] Development of a long-lifetime *monolithic* ceramic molar crown has proved especially elusive. Reported clinical failure rates range from 4% to 6% per year for Dicor molar crowns[2,3] and 3% to 4% per year for Empress crowns.[4,5] In practice, all-ceramic crowns are usually fabricated into *layer* structures with esthetic but weak veneer porcelains on stiff and strong ceramic support cores. Failure rates of InCeram and Procera (Nobel Biocare, Goteborg, Sweden) layer all-ceramic crowns are reportedly lower (1% to 2% per year).[6,7] However, even these rates are unacceptably high relative to metal-core crowns.[8]

Figure 1 illustrates the nature of the problem: a molar crown has fractured after only 2 years in the mouth, by propagation of an occlusal-to-gingival crack that extends across the entire crown. There is a need to understand the fundamental mechanics of failure in layered dental ceramics under loading conditions that represent basic occlusal function. The traditional, empiric approach is to simulate oral function on stylized crowns with mouth motion machines[9] or to use finite element modeling to conduct stress analyses of analogous crown structures. However, such approaches are limited to case studies and provide little insight into the essential relations between the critical loads for damage onset and underlying variables.

Hertzian contact testing with spherical indenters (representing opposing enamel contact) in normal loading on model flat-layer structures (representing crown on dentin) may provide an ideal starting point for understanding such relations at a fundamental level. Such testing has proven particularly powerful in identifying damage modes in ceramic materials, in both monolith and layer forms, for several decades.[10] These modes are depicted schematically in Figure 2. The indentation approach allows simplicity in testing, enabling economic characterization of a wide range of clinically relevant ceramic-based structures without resorting to the empiric time-consuming protocols referred to above. In monoliths, such testing has facilitated the study of 2 competing near-surface damage modes (Fig. 2, *A* and *B*): cone cracking ("brittle" mode) and microdeformation yield ("quasiplastic" mode).[11] Recent extension of Hertzian contact testing to flat bilayer and trilayer structures with ceramic top layers has revealed a different kind of fracture mode

---

Presented before the 50th Anniversary Meeting of the American Academy of Fixed Prosthodontics, February 2000, Chicago, Ill.
This study was supported by a grant from the U.S. National Institute of Dental Research, NIDR Grant PO1 DE10976.
Information on product names and suppliers in this article is not to imply endorsement by NIST.
[a]Fellow, Materials Science and Engineering Laboratory, National Institute of Standards and Technology.
[b]Graduate Student, Department of Materials and Nuclear Engineering, University of Maryland.
[c]Professor, Department of Prosthodontics and Biomaterials, Dental School, University of Medicine and Dentistry at New Jersey.

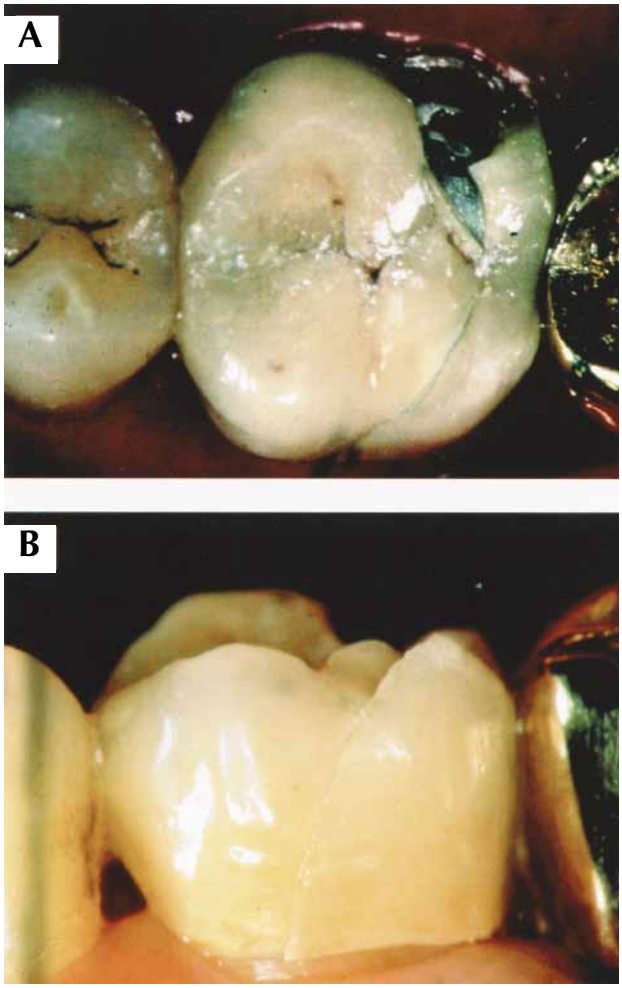

Fig. 1. Example of failure of all-ceramic InCeram molar crown after 24 months, resulting in loss of occlusal-lingual wall and cracked buccal wall. **A,** occlusal view; **B,** buccal view. Photographs courtesy of Suzanne Scherrer (Department of Prosthodontics, School of Dental Medicine, University of Geneva, Geneva, Switzerland).

that can lead to premature failures.[12] This fracture takes the form of "radial" cracks that initiate within thin ceramic layers at the lower crown cementation surface beneath the contact (Fig. 2, *C*) and spread laterally outward along this internal surface. Such cracks are believed to be responsible for crown failures of the type shown in Figure 1.[8]

In unfavorable instances, critical loads for any one of the above damage modes can fall well below the 100 N typical of mastication forces on molar crowns.[13] The manner in which the various damage modes evolve with time after first appearance determines the "damage tolerance" of the crown structure; in multilayer structures especially, damage processes tend to confine themselves to the layer in which they initiate, restricting spread to the remaining tooth structure. Nevertheless, the onset of any form of damage inevitably compromises the strength of the structure and signals an effective end to useful lifetime. One major advantage of controlled contact testing is that simple analytic relations may be derived for the critical loads in terms of basic material properties (modulus, hardness, toughness, strength), layer thickness, and indenter radius. Elements such as complex repeat loading, convoluted tooth geometry, and aqueous oral environment exacerbate the issue. These elements may be added step by step within a contact testing framework to develop a comprehensive model of crown behavior.

In this review article, existing knowledge of contact damage modes in crownlike flat-layer structures is surveyed, beginning with monolithic ceramics and progressing to more complex ceramic layers on compliant substrates. Principal damage modes in these structures are identified and analyzed, following the scheme depicted in Figure 2. The issue of competing cone cracking and quasiplasticity modes in monolithic or thick ceramic layers is addressed first. Model experiments that enable direct observation of the evolution of the dangerous radial cracks in simple ceramic/dentinlike bilayer structures then are described, and critical load data from these experiments are presented for selected dental ceramics. Fundamental relations for the critical loads in terms of material and geometric parameters are put forward, and crown design concepts evolving from these relations are discussed. Consideration is given to the role of flaws at the upper and lower ceramic surfaces (corresponding to "superior" and "inferior" crown surfaces) on the strengths of layer structures, with the use of controlled abrasion flaws in simulated dental preparation procedures. Finally, new work on trilayer veneer/core/dentinlike systems is described.

MONOLAYER CERAMICS

Table I lists basic mechanical data for selected representative dental ceramics as well as for pertinent substrate and indenter materials, model test materials, and natural tooth materials. The properties listed—Young's modulus (*E;* resistance to elastic deformation), hardness (*H;* resistance to plastic deformation), toughness (T or K_{IC}; resistance to crack propagation), and strength (σ; maximum sustainable tensile stress)—are routinely measured on monolithic specimens in materials laboratories. As will be demonstrated, these basic properties determine damage responses in given ceramic structures from contacts with curved indenting surfaces.

Following the scheme of Figure 2, the review begins with a characterization of damage in monolithic ceramics from indentation with hard spheres (usually tungsten carbide [WC]) of a prescribed radius

on polished specimen surfaces. This appears to be an essential first step in any attempt to understand the corresponding properties of ceramic-based layer structures. Near-contact damage modes in monolith specimens provide useful upper bounds to the occlusal forces sustainable by prospective ceramic veneer crown systems.

Contact relations

Consider a spherical indenter in elastic contact with a flat monolith half-space (Fig. 2, *A*). From the classical Hertzian equations,[14] the mean contact pressure p_0 at normal load P is[10]

$$p_0 = [4E/(3\pi^{3/2})(1 - \nu^2)r]^{2/3}P^{1/3} \quad (1)$$

where ν is the Poisson ratio, r an "effective radius," and E an "effective modulus"

$$1/r = 1/r_c + 1/r_i \quad (2a)$$

$$1/E = 1/E_c + 1/E_i \quad (2b)$$

where subscripts c and i denote ceramic and indenter materials, respectively. This formulation accounts for indenters of different modulus and specimens of different curvature. Thus, for rigid indenters on flat specimens, $r = r_i$ and $E = E_c$; for like indenters and specimens (enamel opposing enamel, for example), $r = r_i/2$ and $E = E_c/2$. At any given load P, the contact pressure p_0 is the same for these 2 illustrative examples, suggesting that tests with hard indenters on flat-layer specimens are indeed representative of cuspal contacts.

Cone crack and quasiplasticity damage modes

Beyond some critical load, the elastic limit of the material is exceeded and irreversible damage occurs beneath the spherical indenter. Special sectioning techniques have been developed for examining subsurface damage, including a particularly useful "bonded-interface" technique in which the specimen is split and rejoined before indentation and the ensuing damage is viewed in Nomarski illumination after the separated surfaces have been gold-coated.[15,16] Two basic damage modes have been identified (Fig. 2, *A*): brittle and quasiplastic. In the former, classical brittle (tensile-driven) single "cone" cracks initiate from the surface[17,18]; in the latter, distributed (shear-driven) microcracks initiate within a subsurface "yield" zone.[11,16,19] The brittle mode has been studied for more than a century[10,20] and occurs mainly in brittle glasses, brittle porcelains, and fine-grained ceramics. The quasiplastic mode has only recently been documented[1] and occurs most prominently in coarse-grained, tougher ceramics such as aluminas and zirconias.

An example of each mode is illustrated in Figure 3 for a micaceous glass-ceramic indented with WC spheres. In this material, the grain size is controlled by varying the temperature during the crystallization heat treatment.[21] The fine-grained forms show dominant cone cracking (Fig. 3, *A*), whereas the coarse-grained forms show dominant quasiplasticity (Fig. 3, *B*). The dental material Dicor originates from this family of glass-ceramic and actually lies somewhere between the 2 extremes represented in Figure 3.[22] Both damage modes evolve further in cyclic loading[23]: the brittle mode by slow extension of the cone crack; and the quasiplastic mode

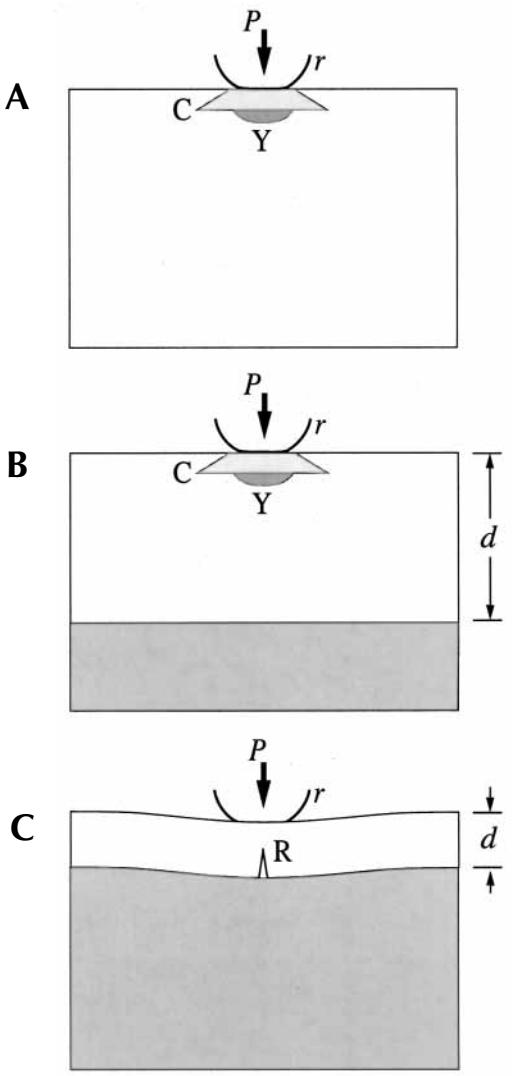

Fig. 2. Schematic of damage modes in flat ceramic material of layer thickness d from indentation with sphere of radius r at load P. **A,** Ceramic monolith: contact induces either cone cracks (brittle mode) or yield zone (quasiplastic mode) in top surface region. **B,** Bilayer, thick ceramic layer on thick compliant substrate: brittle and quasiplastic modes remain dominant. **C,** Bilayer, thin ceramic layer on thick compliant substrate: ceramic flexes and subsurface radial cracks initiate from ceramic/substrate interface and spread upward and outward.

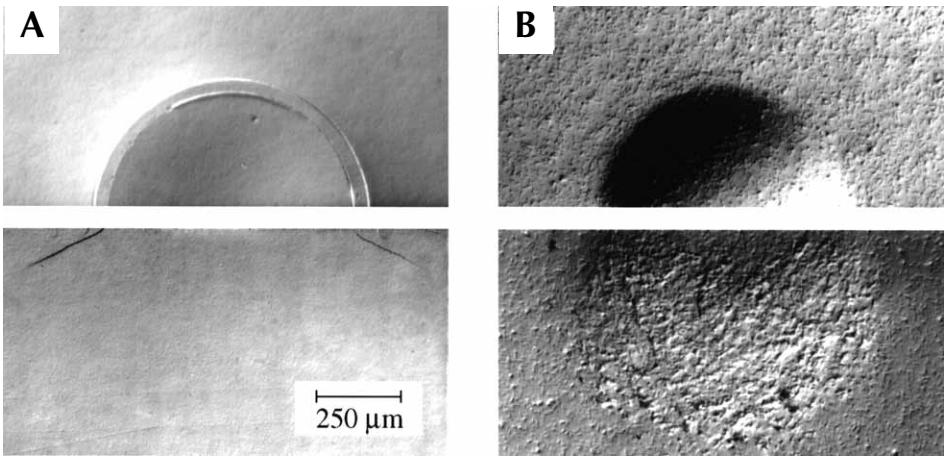

Fig. 3. Damage in fine-grained **(A)** and coarse-grained **(B)** micaceous glass-ceramic from indentation with WC sphere of radius r_i = 3.18 mm at load P = 1000 N. (Dicor comes from same composition and lies between these two extremes.) Upper micrographs are half-surface views and lower micrographs side views from bonded-interface specimens.[51]

by relatively rapid microcrack coalescence, leading ultimately to formation of subsurface radial cracks. These cracks can seriously degrade the strength of the ceramic,[24] especially in cyclic loading in aqueous environments.[23,25-28] Quasiplasticity-induced radial cracks may develop even in the most brittle dental ceramics,[23,28,29] as demonstrated in Figure 4 for Mark II dental porcelain subjected to cyclic contact in water.

Critical loads

Considerable effort has been expended to develop analytic expressions for the critical loads to initiate each near-contact damage mode with sphere indentation. For cone cracks, the critical load for single-cycle loading is[10,17,30]

$$P_C = A(T_c^2/E)r \quad (3)$$

where A is a dimensionless coefficient and T_c is the toughness of the ceramic (commonly termed K_{Ic} in the engineering fracture community). Toughness arises as a controlling parameter in this equation because the cone crack first develops as a surface ring and then propagates stably before full cone crack initiation—and it is toughness that determines the resistance to crack propagation. For quasiplasticity, the corresponding critical load is[30]

$$P_Y = DH_c(H_c/E)^2 r^2 \quad (4)$$

where D is another dimensionless coefficient and H_c is indentation hardness (load/projected area, Vickers indentation) of the ceramic. Hardness appears because it is a yield process that determines the intensity of shear stress responsible for activating the quasiplasticity mode. Fits of these relations to critical load data for ceramics of which the basic properties are well known enable coefficient evaluations $A = 8.6 \times 10^3$ and $D = 0.85$.[30] Sphere radius r appears explicitly in Equations 3 and 4, reflecting the important role of near-contact conditions.

These relations enable a priori calculations of critical loads for each damage mode, for any given prospective ceramic, and at any prescribed effective sphere (opposing cuspal) radius. In Fig. 5, plots of P_C and P_Y are shown for selected ceramics as a function of composite parameters T_c^2/E and $H_c(H_c/E)^2$, respectively, with parameters from Table I. The calculations are for like opposing contacts ($r = r_i/2$ and $E = E_c/2$), for values of r within a clinically relevant range of 1 to 10 mm, including a midrange value r = 3.18 mm. The adequacy of any given material may be considered relative to a nominal occlusal force P = 100 N (Fig. 5, dashed horizontal line). On this basis, it would appear that most ceramics are unlikely to sustain cone cracking, though Mark II porcelain and Dicor at the lower end of the plot are susceptible at low r. All the ceramics represented, but most notably the glass-ceramics, are susceptible to quasiplasticity at low r. The interchange between Empress I and Empress II in the 2 diagrams is noteworthy. Clearly, prevention of these damage modes, especially near-contact quasiplasticity, requires avoidance of sharp contacts.

CERAMIC-BASED BILAYERS

As alluded to above, characterization of the damage properties of flat-surface monolithic ceramics is an essential first step in understanding the behavior of layer structures. Then it is simply a case of investigating the role of a soft supporting underlayer on the damage modes in the brittle ceramic overlayer (Fig. 2). Several studies of this kind, mostly with ceramic plates

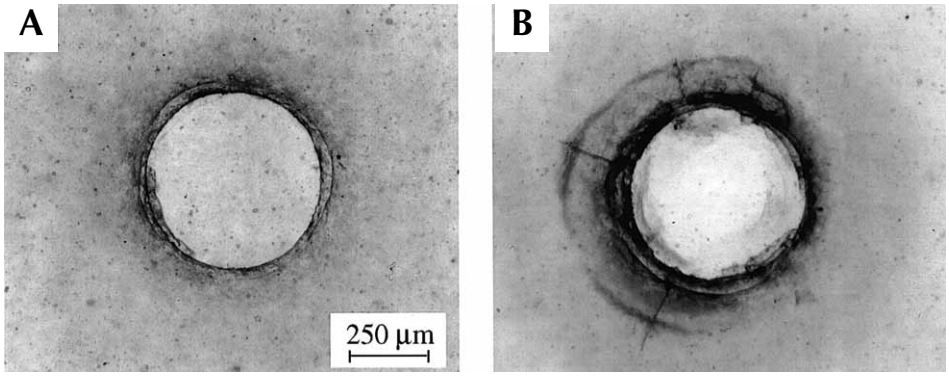

Fig. 4. Damage in Mark II feldspathic porcelain from indentation with WC sphere of radius r_i = 3.18 mm at load P = 500 N, in water. Top-surface views: single-cycle **(A)** and 5×10^3 cycles **(B)**. Note initial cone crack and subsequent radial cracks.[26]

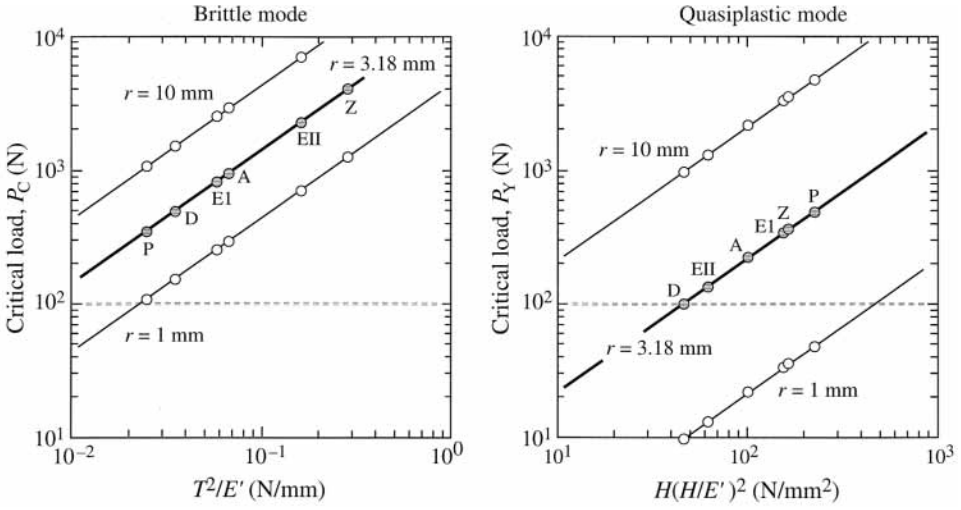

Fig. 5. Calculated critical loads P_C and P_Y as a function of appropriate material parameters for selected dental ceramics: *P* = Mark II porcelain; *D* = Dicor; *EI* = Empress porcelain; *EII* = Empress II glass-ceramic; *A* = alumina (infiltrated); *Z* = Y-TZP zirconia. Plots at indicated values of cuspal radius *r* for like material contacts. Generally, except for porcelain, critical loads for quasiplasticity tend to be lower than those for cone cracking.[13]

cemented to dental resin composite substrates, have been reported in the dental literature.[8,31-34] Parallel studies of flat ceramic coating systems on a broad variety of substrates have been reported in the materials literature.[35-41] These studies identify radial cracking at the lower ceramic surface (interestingly, not delamination at the ceramic/substrate interface) as a major fracture mode in crownlike ceramic layer structures. The same studies identify the source of radial cracking with flexure of the ceramic layer on a compliant substrate (rather than with a buildup of quasiplasticity, as described in the previous section). However, until recently, the fundamental relations among critical load, material parameters, and layer thickness have remained obscure.

Accordingly, in this section, extensions of the contact testing methodology for monolithic ceramics to ceramic-based bilayer (monolithic crown) structures are explored. For the purpose of elucidating fundamental damage relations, it is useful to employ model flat-surface structures, including some with constituent transparent layers to enable in situ observation of the radial cracking mode. Once the protocol is established for bilayers, the cornerstone is laid for further extensions to trilayer (veneer/core crown) structures.

Radial cracks in model bilayer structures

The motivation behind the use of model flat-surface bilayer structures is elucidation of the

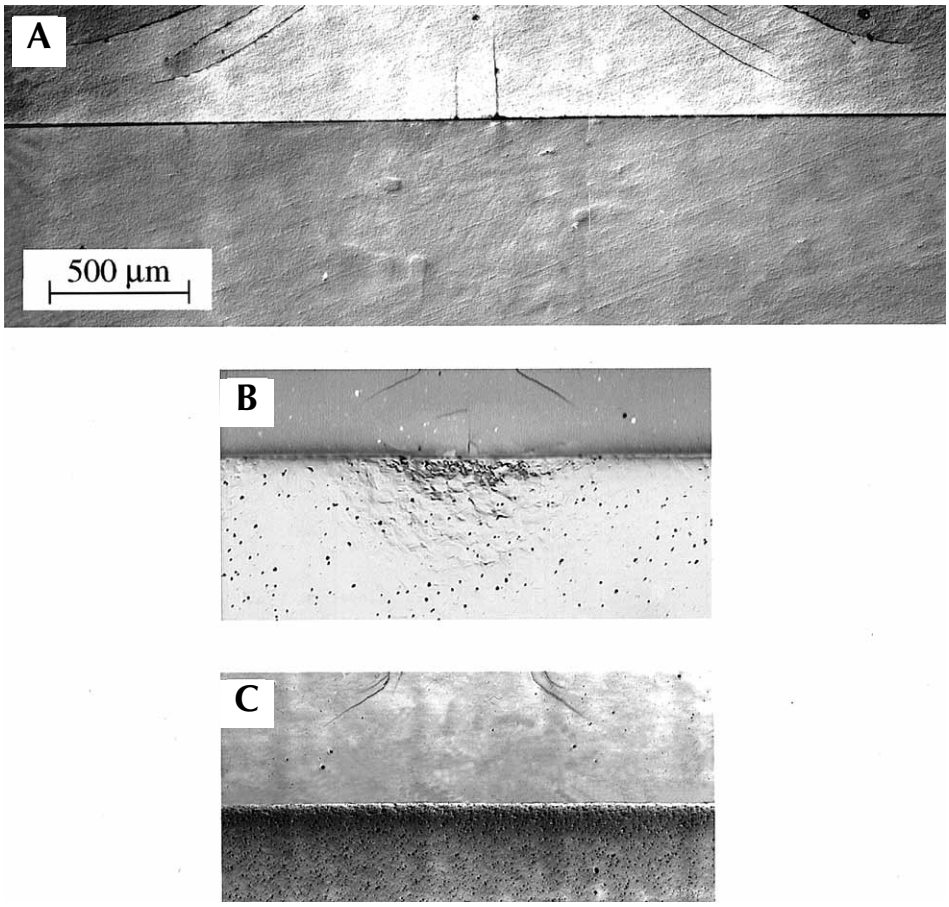

Fig. 6. Section views of cracking in flat ceramic/substrate bilayers. **A,** Glass-ceramic/filled-polymer, ceramic thickness $d = 0.45$ mm, WC sphere indenter $r_i = 3.18$ mm at $P = 450$ N.[39] **B,** Porcelain/Pd-alloy, $d = 0.45$ mm, $r_i = 2.38$ mm at $P = 500$ N.[43] **C,** Porcelain/glass-infiltrated-alumina, $d = 0.50$ mm, $r_i = 3.18$ mm at $P = 500$ N.[39] Bonded-interface specimens.

mechanics of radial crack evolution, with minimum complication. Routine specimen preparation and simple testing procedures are desirable for this purpose. Accordingly, ceramic layers are joined to dentinlike substrates by interfacial fusing (according to manufacturers' specific heating schedules, notably for porcelain) or by luting with dental cement or epoxy adhesive. Contact testing is performed on polished upper ceramic surfaces with spherical indenters in the same way as with monoliths. Subsurface damage is examined either after testing with bonded-interface techniques[41] or during testing by in situ observation through transparent layers.[42]

Three examples of contact-induced damage in bonded-interface bilayer specimens fabricated from dental materials are illustrated in Figure 6: Dicor-like glass-ceramic bonded with dental cement to a filled-polymer composite substrate,[41] porcelain fused to Pd-alloy metal,[43] and porcelain fused to glass-infiltrated alumina.[41] In all these instances, the elastic modulus of the upper ceramic material is comparable to tooth enamel (Table I). The elastic modulus of the filled-polymer substrate is relatively small (approximating that of dentin); it is relatively high for the other 2 substrate materials, especially in the alumina, typical of ceramic crown core materials.

The contact loads used in Figure 6 are well in excess of a nominal biting force of 100 N, so the damage modes are well developed. Cone cracks are apparent in all 3 examples; however, whereas in Figures 6, *B* and *C,* the cone geometry closely resembles that in monoliths (Fig. 3, *A*), the cone diameters in Figure 6, *A,* are much wider. The latter is attributable to enhanced flexure of the ceramic plate on the softer polymeric substrate, which shifts the maximum surface tensile stress from the edge of the near contact to the outer shoulders of the deflecting plate.[42] Upward extending radial cracks are especially apparent in this system, indicating concurrent development of substantial tensile stresses at the lower plate surface.[35,40,42] Radial cracks are also evident in the porcelain on metal substrate in Figure 6, *B,* notwithstanding the higher substrate stiff-

Table I. Properties of dental materials*

Material	Name†	Supplier†	Function	Modulus *E* (GPa)	Hardness‡ *H* (GPa)	Toughness *T* (MPa · m1/2)	Strength σ (MPa)
Ceramic							
Porcelain	Mark II	Vita Zahnfabrik (Bad Sackingen, Germany)	Veneer	68	6.4	0.92	130
	Empress I	Ivoclar (Schaan, Liechtenstein)	Full crown	67	5.6	1.4	160
Glass-ceramic	Dicor	Dentsply (York, Pa.)	Full crown	69	3.8	1.1	320
	Empress II	Ivoclar	Full crown	104	5.5	2.9	420
Alumina (infiltrated)	InCeram	Vita Zahnfabrik	Ceramic core	270	12.3	3.0	550
Zirconia (Y-TZP)	Prozyr	Norton (East Granby, Conn.)	Ceramic core	205	12.0	5.4	1400
Glass	Soda-lime		Model material	73	5.2	0.67	110
Glass-ceramic	MCG (fine)	Corning (Corning, N.Y.)	Model material	70.5	3.8	1.0	325
	MCG (coarse)	Corning	Model material	51.5	2.7	1.65	125
Sapphire	Single crystal	Goodfellow Ltd (Cambridge, England)	Model material	417	21.0	3.0	550
Metal							
Pd-alloy	Argipal	Argen Precious Metals (San Diego, Calif.)	Metal core	126	2.0		
Tungsten carbide	Kennametal	J & L Industrial (Livonia, Mich.)	Indenter	614	19.0		
Polymer							
Polycarbonate	Hyzod	AIN Plastics, Inc (Virginia Beach, Va.)	Substrate	2.3	0.15		
Filled polymer	Charisma	Hereaus Kulzer GmbH (Wehrtheim, Germany)	Substrate	10	0.8		
Epoxy	RT Cure	Master Bond Inc (Hackensack, N.J.)	Adhesive	3.5	0.9		
Tooth							
Enamel			Natural tooth	94	3.2	0.8	
Dentin			Natural tooth	16	0.6	3.1	

*Data courtesy I. M. Peterson, J. Quinn, H. Xu, and Y. W. Rhee. Uncertainties estimated at 5% in *E*, 10% in *H*,15%-20% in *T*, and 15-20% in σ
†Information on product names and suppliers in this paper is not to imply endorsement by NIST.
‡Calculated as indentation hardness, $H = 2P/a^2 = 1.078H_V$, *a* = indent diagonal.

ness. In this instance, the metal has a lower hardness than the porcelain (Table I), which facilitates substrate yield below the contact. The yield locally deforms the support with resultant deflection of the ceramic and radial crack initiation.[35,36] No such radial cracking is evident in Figure 6, *C;* the combined high stiffness and hardness of the alumina provides a much more rigid support. These observations appear to favor stiff and hard ceramics like alumina for substrate materials. It will be shown that such conclusions do not extend unequivocally to the design of crownlike trilayers.

Although bonded-interface and other postindentation sectioning specimens are useful in identifying damage modes, they provide only limited information. They are not readily amenable to determination of out-of-plane crack extension or to quantitative evaluation of critical loads. In addition, they are subject to certain artifacts.[44] Acoustic detection may be used to detect the onset of cracking in some opaque ceramics, but even if measurable signals are obtainable, it is not always easy to determine which crack forms first or to follow the ensuing crack evolution. In an effort to overcome these limitations, model crown/dentin layer structures have been constructed with representative transparent substrates to allow direct in situ viewing during loading and unloading.[42,45]

An example from a video sequence of crack evolution during contact loading is shown in Figure 7 for a thin alumina plate bonded to a polycarbonate substrate with a thin (≈10 μm) interlayer of epoxy adhesive.[13] Here, the alumina is prepared by glass infiltrating a preform,[24] analogous to the InCeram process. The frames in Figure 7 show the radial crack immediately after critical load *(A)*, ensuing stable crack propagation and multiplication with increasing load (*B* through *D*), and crack closure (but not healing) on unloading (*E* and *F*). Comparative in situ side views in specimens with transparent ceramic (glass)

layers[42] indicate extensive lateral propagation of the radial cracks over distances several times the ceramic thickness, without penetration to the upper surface. (Natural teeth have this capacity to sustain subsurface cracks without imminent failure, indicating a certain damage tolerance.) Nevertheless, first cracking severely compromises the specimen strength and may be regarded as signaling an end to useful lifetime. Ultimately, at loads typically a few times that required for initiation, penetration does occur, resulting in specimen failure.

Critical loads

The Hertzian relations for a sphere in contact with a ceramic of modulus E_c (mean pressure in Eqn. 1) will inevitably be modified by the presence of an underlayer of different modulus E_s, to an extent dependent on the ceramic thickness d.[46] For large d, any such modification will be minor, so that near-surface damage (cone cracking or quasiplasticity) will remain dominant damage modes (Fig. 2, *B*). In this limit, the critical load relations in Equations 3 and 4 remain adequate approximations. For small d, the modification may radically alter the basic nature of the stress field in the ceramic plate, facilitating flexure and so shifting stress maxima away from the contact surface to the subsurface. Radial cracking at the lower ceramic surface then becomes the principal mode of damage (Fig. 2, *C*), necessitating entirely new relations for the critical load.

For a thin ceramic plate on a low-modulus substrate (Fig. 6, *A*), the basis for analysis of radial fracture may be found in classical elasticity solutions for the stresses in surface-loaded flexing plates on compliant foundations.[14] Equating the maximum tensile stress at the lower surface of such a plate to the strength (σ_c) of the component ceramic material yields an explicit relation for the critical load[13,42]

$$P_R = B\sigma_c d^2/\log(E_c/E_s) \quad (5)$$

where B is a dimensionless coefficient. The logarithmic modulus term in this relation was foreshadowed by Scherrer et al,[32] but the dependence on thickness d remained elusive.[8,34] Fits of Equation 5 to critical load data for model glass/substrate systems yield a coefficient evaluation $B = 2.0$.[12] At $P = P_R$, the radial crack "pops in" to its elongate geometry, with lateral dimension $c \approx d$ and through-thickness dimension $c \approx 0.5d$.[47] With an increase in P beyond P_R, the crack expands stably, continuing in its elongate geometry, until it ultimately penetrates to the upper surface.

In the example of a thin ceramic plate on a stiff but soft metal substrate, radial cracking may occur as a result of yield in the metal (Fig. 6, *B*). Yield is now an essential precursor to plate flexure; strictly, therefore, a full solution requires a nonlinear elastic–plastic analysis. A simplifying approach is to take the critical load P_Y for first metal yield as a working lower bound ($P_Y < P_R$), so that elasticity solutions may be retained to determine the critical condition. The ensuing relation for the critical load is[48]

$$P_Y = GH_s d^2 \quad (6)$$

where H_s is the hardness of the substrate, $G = G(E_c/E_s) = \alpha + \beta E_c/E_s$ is a modulus mismatch factor, and α and β are dimensionless coefficients (compare with Eqn. 4 for quasiplasticity in monoliths). A numerical evaluation yields $\alpha = 0.57$ and $\beta = 0.17$.[48] The recurrence of the quadratic d^2 term in Equation 6 (compare with Eqn. 5) is reflective of flexural stress solutions for plates and beams.[14] The appearance of H_s in this equation indicates that palladium and other hard base metal alloys will have a clinical advantage over gold alloys at any given porcelain thickness.

Unlike the cone crack and quasiplastic relations for monoliths (Eqns. 3 and 4), Equations 5 and 6 contain no term in sphere radius r. This is because the radial cracks (or substrate yield) form remote from the surface in the far field of lower-surface flexural stresses, so details of the contact conditions (occlusal area, for example) are unimportant. Experimental confirmation of this null dependence has been obtained in measurements of P_R on glass/polymer bilayers over a wide range of sphere radius.[13]

Crown design diagrams

The critical load relations defined above enable construction of design diagrams for prospective monolithic crown systems.[12,30,42,43] The concept is illustrated in Figure 8 as a plot of critical load for the onset of first damage as a function of layer thickness d for model flat-layer ceramic/polycarbonate bilayers (Fig. 2) at fixed sphere radius $r_i = 3.96$ mm. Filled symbols are P_R data for radial cracking; unfilled symbols are P_C data for cone cracking ($P_C < P_Y$) or P_Y data for quasiplasticity ($P_Y < P_C$) in the ceramic layer. Solid lines (and their dashed extensions) are a priori predictions from Equations 3 through 5 in conjunction with the material parameters in Table I. In the thicker ceramic layers ($d \geq 1$ mm), first damage initiates from the ceramic top surface as cone cracks in porcelain but as quasiplasticity in the other ceramics. In the thinner layers ($d \leq 1$ mm), radial cracks initiate first. The load P_R is highly sensitive to d, covering more than 2 orders of magnitude over the thickness range investigated. The relative positions of the $P_R(d)$ data for the different ceramics are commensurate with the strength values in Table I, suggesting that plots of this kind may be useful for ranking materials for damage resistance. Recall that the positions of the $P_R(d)$ curves are independent of sphere radius r_i, but the P_C or P_Y plateaus will be depressed at lower r_i (Fig. 5).

An analogous plot is shown in Figure 9 for model

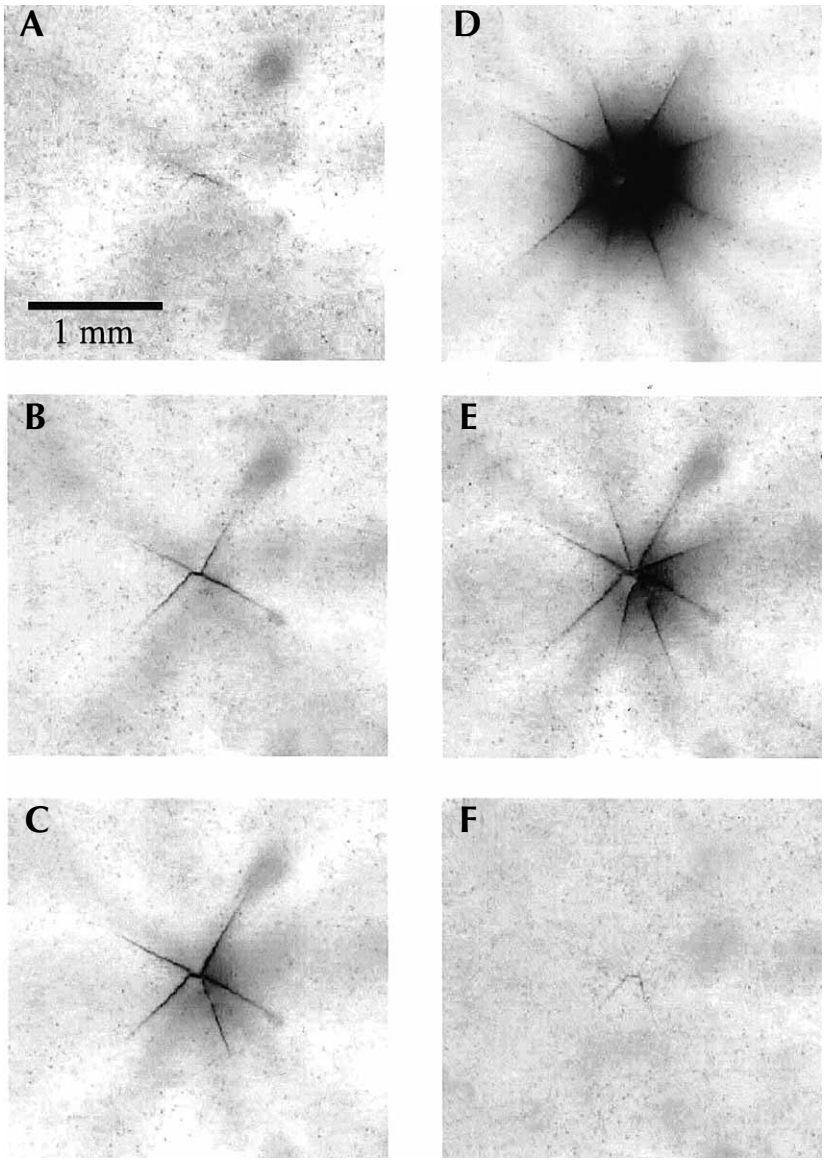

Fig. 7. In situ subsurface views of radial crack sequence at lower as-polished surface of alumina outer layer; thickness d = 0.15 mm, on polycarbonate substrate, from indentation with WC sphere, r_i = 3.96 mm. Loading half cycle: P = 15.1 N **(A)**, P = 24.0 N **(B)**, P = 35.1 N **(C)**, and P = 56.6 N **(D)**. Unloading half-cycle: P = 33.3 N **(E)** and P = 0 N **(F)**.[13]

porcelain/Pd-alloy bilayers (Fig. 6, *B*). In this instance, filled symbols represent P_Y data for substrate yield and unfilled symbols represent P_C data for porcelain cone cracking. Solid curves are predictions from Equations 3 and 6 with parameters from Table I. Again, the danger exists for radial cracking to occur in thin porcelain layers ($d \leq 0.4$ mm).

These results demonstrate how changes in ceramic and substrate materials, as well as in layer and sphere dimensions, may influence critical loads for the onset of damage. For any given system, the aim is to remain below the envelope of solid curves in the figures. This places practical restrictions on the layer thickness d and contact radius r. The critical load relations of Equations 3 through 5 now can be used to predict the responses for any given ceramic/dentin system in dental function. Real ceramic crowns are generally cemented directly onto underlying tooth dentin, so the substrate modulus is predetermined (E_s = 16 GPa[49,50]); and the "indenter" is the opposing tooth, with fixed enamel modulus (E_i = 94 GPa) and with cuspal radius $r_i \approx r_c$ in Equations 1 and 2.

Suppose that the maximum tolerable biting force is P_m = 100 N. This load corresponds to critical dimensions below which damage will be sustained: r_C (cone cracking, $P_m = P_C$ in Eqn. 3), r_Y (quasiplasticity, $P_m = P_Y$

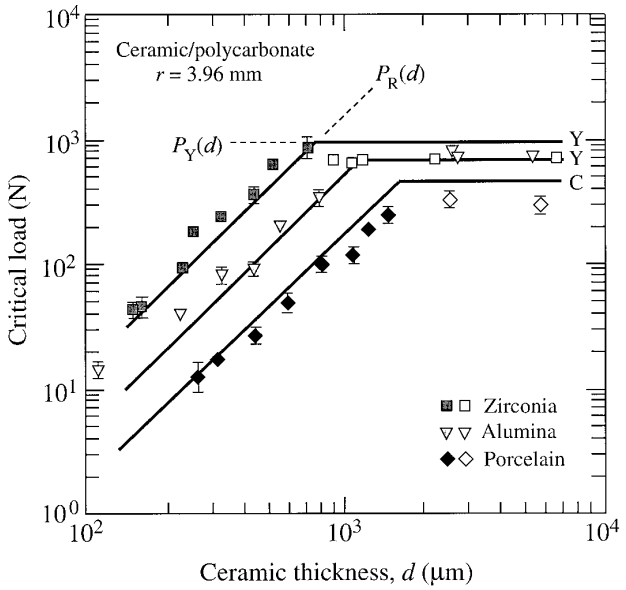

Fig. 8. Critical loads for first damage in ceramic/polycarbonate bilayers as function of coating thickness d for indentation with WC spheres of r_i = 3.96 mm. *Filled symbols* are P_R data; *unfilled symbols* are P_C and P_Y data. *Error bars* are uncertainty bounds. *Solid lines* are theoretical predictions for radial and cone cracking *(C)* and quasiplasticity *(Y)*.[13]

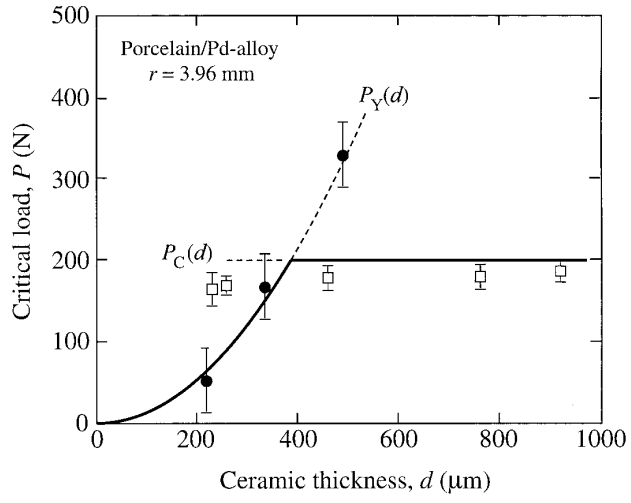

Fig. 9. Critical loads for initiating damage in ceramic/Pd-alloy bilayers as function of coating thickness d for indentation WC spheres of r_i = 3.96 mm. *Filled symbols* are P_Y data; *unfilled symbols* are P_C data. Critical load P_Y foreshadows initiation of radial cracks ($P_Y < P_R$). *Solid lines* are theoretical predictions for porcelain cone cracking and metal yield.[43]

in Eqn. 4), and d_R (radial cracking, $P_m = P_R$ in Eqn. 5). Figure 10 plots these critical dimensions for selected dental ceramics. Shaded areas are representative clinical operating domains. The design objectives are to avoid sharp contacts and thin layers—namely, to ensure that r_C and r_Y lie below a minimum operating radius (nominal 2 mm) and that d_R lies below a minimum operating layer thickness (nominal 1 mm). It would appear in Figure 10 that most ceramics are relatively immune to cone or radial cracking, provided the contacts do not become unduly sharp or the ceramic layers unduly thin. However, some ceramics (especially the glass-ceramics) are highly susceptible to quasiplasticity,[51] which is attributable to a relatively low hardness H_c (Table I). This latter susceptibility may contribute to the unacceptably high failure rates of glass-ceramic molar crowns in clinical practice.[2,3]

Role of flaw state

Of special interest in connection with radial cracks in ceramic layers on compliant substrates is the appearance of strength σ_c in Equation 5. Fracture in ceramics invariably begins from some "flaw" in the surface or subsurface. Strength varies with the inverse square root of the size c of this flaw (the celebrated "Griffith relation," $\sigma_c \propto T/c^{1/2}$).[1] In polycrystalline ceramics with coarser grained structures and gross defects (especially voids), such flaws are intrinsic to the microstructure.[51] For homogeneous glasses or ceramics with fine microstructures, large extrinsic flaws may be introduced during surface handling or shaping (sandblasting, grinding, or machining). In these latter materials, strength may be systematically varied by abrading the top surfaces with abrasive grits of different sizes.[42,52] It therefore would seem advisable to avoid large surface flaws in the brittle-layer internal surfaces during crown fabrication and cementation procedures to prevent reductions in strengths and associated downward shifts of the $P_R(d)$ function in Figures 8 and 10. Corresponding loads P_C in Equation 3 and P_Y in Equation 4 are independent of strength and relatively insensitive to starting flaw size in the top surfaces.[52]

To demonstrate the effect of flaw size on strength, experiments have been conducted on ceramic/polycarbonate bilayers similar to those used in Figure 8, but with large artificial flaws introduced into the ceramic undersurfaces with a Vickers diamond indenter before epoxy-bonding to the polycarbonate substrates.[47] The Vickers indentation produces square-shaped plastic indentations with well-defined cracks emanating from the impression corners, the size of which can be accurately controlled by varying the load.[53] With use of the in situ observation technique described above, the Vickers impressions may be readily centered beneath the spherical indenter in the subsequent Hertzian test, and evolution of the corner cracks can be followed as the load is applied by viewing from below (Fig.

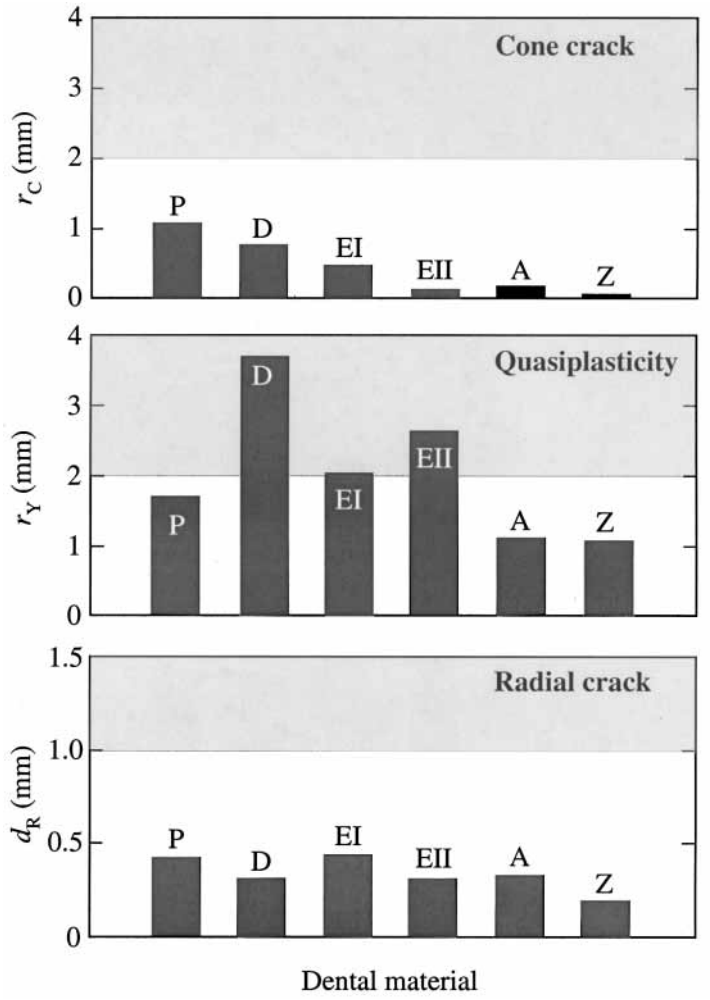

Fig. 10. Plots of critical contact radius for cone cracking *(r_C)* and quasiplasticity *(r_Y),* and critical ceramic layer thickness for radial cracking *(d_R)* at nominal contact force $P = 100$ N. Data for selected dental ceramics (abbreviations listed in Fig. 5). *Shaded area* is clinical "danger zone."

7). Figure 11 plots the critical loads P_R to pop in full radial cracks in ceramic layers of nominal thickness $d = 1$ mm, as a function of the dimension c of the starting Vickers flaws. Filled symbols indicate data for extensions from the Vickers indentation sites themselves; unfilled symbols represent extensions from other (natural flaw) sites. The shaded band indicates a typical size range for extraneous surface flaws introduced by abrasion, machining, or sandblasting treatments.[51] The indication is that such extraneous flaws do not become dominant until they exceed $c \approx 10$ μm. At larger c, P_R declines steadily, suggesting that some ceramics may be considerably degraded in adverse preparation conditions. Interestingly, the decline is less pronounced in the porcelain than in the zirconia and alumina. The relative insensitivity to flaw size in the porcelain may be partly attributable to the dominance of a pre-existent population of large natural flaws (voids, crystalline inclusions)[44,47] over all but the most severe extraneous surface handling flaws, implying that this material may be relatively damage tolerant.

CERAMIC-BASED TRILAYERS

Whereas bilayer structures establish useful starting points for designing all-ceramic dental crowns, the most enduring crown structures are veneer/core/dentin trilayers. Yet studies on trilayer crown systems in the literature are sparse. In precursor studies, White et al[54] and Zeng et al[55] investigated the failure of unsupported all-ceramic porcelain/alumina bilayers in bending and showed that fractures generally occur at the lower alumina surface, even though the strength and modulus of the alumina greatly exceed that of the porcelain. Wakabayashi and Anusavice[56] tested similar porce-

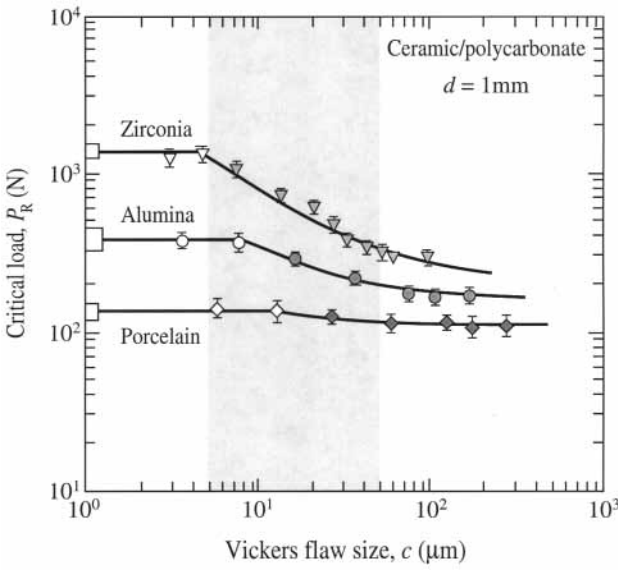

Fig. 11. Critical load (P_R) to produce radial crack pop in from emplaced Vickers indentation flaws of starting size c at lower surface of ceramic plate, thickness d = 1 mm, bonded to polycarbonate substrate. *Filled data* indicate crack pop in from Vickers flaws, *unfilled symbols* from natural flaws. *Open boxes at left axis* are data for unindented specimens. *Error bars* are standard deviations, minimum 5 indentations. *Shaded band* is typical range of surface flaw sizes from abrasive handling procedures (sandblasting, for example).[47]

lain/alumina bilayers but on dentinlike resin substrates; they demonstrated that radial cracking again initiates from the lower core surface (though cone cracks did initiate first in thicker porcelain layers). Unlike in unsupported specimens, where crack initiation was synonymous with total failure, the cracking in the supported specimens remained constrained within the ceramic layers, leaving the composite layer system intact (damage tolerance).

These limited studies suggest the need for further investigations on model veneer/core/resin layer structures to clarify the fracture modes, to elucidate the role of the resin support, and to quantify the critical load dependence on material properties and layer thicknesses.

Model trilayer systems

A recent study has been made of fracture modes in a model transparent trilayer system consisting of glass/sapphire bilayers on polycarbonate substrates.[57] This material system was chosen to simulate porcelain/infiltrated-alumina (InCeram) crowns on dentin. Before assembly of the trilayers, controlled surface abrasion treatments were used selectively to reduce the strengths of the original as-polished glass and sapphire to those of porcelain and alumina (Table I). The layers then were bonded together with a thin layer (≈10 μm) of epoxy adhesive, as in construction of the model bilayers.

Figure 12 shows side views after indentation at the upper trilayer surface with a spherical indenter. The 3 examples represent similar specimens, but each with a different surface abraded: *(A)* top glass surface abraded, with resultant formation of a shallow cone crack in the glass; *(B)* bottom glass surface abraded, with formation of a radial crack in the glass; and *(C)* bottom sapphire surface abraded, with formation of a radial crack in the sapphire. Of the 3 crack systems, the radial crack in the sapphire pops in at the lowest critical load, emitting an audible "ping" as it does so, and spreads over the greatest lateral distance. These latter cracks would clearly threaten the lifetime of a crown structure. It is evident by comparison of Figure 12, *C,* with its bilayer (porcelain/infiltrated-alumina) counterpart in Figure 6, *C,* that the radial cracks are facilitated by deflection of the compliant substrate. However, all cracks are fully confined within their originating layers, attesting to the capacity of the substrate to constrain the spread of damage. In particular, the substrate remains intact, so the fracture is not immediately catastrophic.

Analytic relations for the critical loads to initiate radial cracks in trilayers, analogous to those for bilayers above, are not yet available, necessitating resort to numeric analysis. Finite element computations shown in Figure 13 indicate stress distributions for the model glass/sapphire/polycarbonate system in Figure 12 at the critical load for radial cracking in the sapphire.[57] The plot shows contours of the tensile stress normal to the radial crack plane for 2 examples: *(A)* with 10-μm interlayer adhesive; and *(B)* without interlayer adhesive (but well bonded, corresponding to a fused veneer/core interface). Maxima in tensile stresses in both the glass and sapphire layers occur at the bottom surfaces along the contact axis. It is apparent that the bulk of the load has been transferred from the glass to the sapphire, typical of flexing bilayers with low-modulus upper members.[54] Thus, although the veneer (glass, porcelain) is much weaker than the core (sapphire, alumina), the stiff core is most vulnerable. Removing the glass/sapphire adhesive interlayer eliminates any tensile stress in the glass[45] but does not strongly disturb the stress contours at the sapphire lower surface. The pronounced lateral spread in the contours along the bottom surface of the sapphire layer and confinement of the tensile stresses to the bottom portion of this layer are consistent with the crack geometry seen in Figure 12, *C.* Finite element calculations such as those in Figure 13 can be used to evaluate critical loads (by equating the maximum tensile stress in each layer to the appropriate

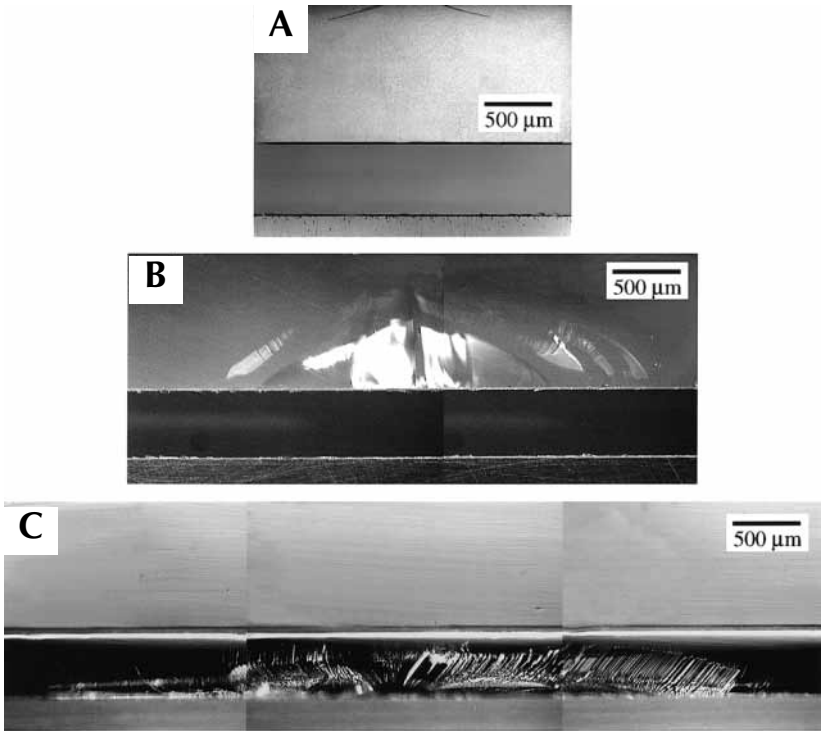

Fig. 12. Crack profiles in trilayer of glass/sapphire "crown." Thickness d_g = 1.0 mm and d_s = 0.5 mm, on polycarbonate substrate, after contact with WC sphere, r = 3.18 mm. **A,** Cone crack in top-abraded glass surface, P = 700 N. **B,** Radial crack in bottom-abraded glass, P = 800 N. **C,** Radial crack in bottom-abraded sapphire, P = 430 N.[57]

material strength) and to construct design diagrams (Fig. 10) for predicting the responses of more realistic crown systems.[57]

Analogous experiments are currently being conducted on glass/metal/polycarbonate trilayers in an attempt to determine the reason porcelain-fused-to-metal crowns may last longer than all-ceramic crowns. In these systems, radial cracks are confined to the upper glass (porcelain) layers (Fig. 6, *B*); the issue becomes one of enhanced shear stress in the metal from flexure on the compliant substrate.

SUMMARY

This article has attempted to describe how experiments on model flat-layer structures can provide rare physical insight into failure modes in all-ceramic dental crowns. It is argued that simple contacts with spherical indenters in normal loading constitute a uniquely simple and powerful route to the investigation of such failure modes and yet, at the same time, remain representative of the most basic elements of occlusal function. Damage modes identified include cone cracks and quasiplastic yield zones at the contact surfaces of thicker ceramic crown structures. But a more dangerous mode is interior radial cracking at the lower surfaces of thinner ceramic crown structures. The latter cracks can extend subsurface over relatively long distances, are subject to additional extensions in any subsequent loading, and may ultimately extend to specimen edges or even penetrate to upper surfaces. What makes radial cracks iniquitous is the difficulty of detecting them in postcontact surface inspections in opaque or translucent dental materials. It is in the context of this last point that experimentation on model systems with transparent layers is particularly attractive.

A central goal of the materials approach to the characterization of clinically relevant layer structures in occlusal contact loading is the development of analytic relations for critical loads to initiate the various damage modes. This article has described such relations for flat monolith ceramics and ceramic/soft-substrate bilayers. The relations presented as Equations 1 through 6 are explicit in their dependence on material parameters (elastic modulus, hardness, toughness, and strength) and geometric parameters (ceramic layer thickness and contact radius). In Equation 5, for radial cracks in bilayers, the primary parameters are strength σ_c (linear dependence) and layer thickness d (quadratic dependence) of the ceramic; elastic modulus is of secondary importance, appearing only as a slow (logarithmic) term in E_c/E_s. These primary dependencies have not previously been confirmed in the dental literature.

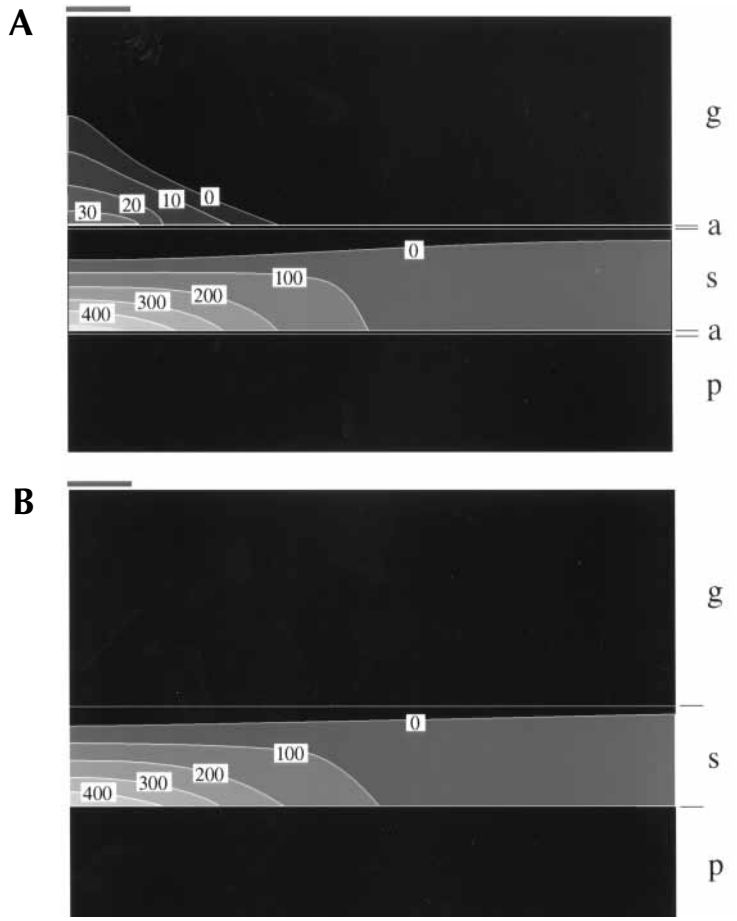

Fig. 13. FEM-generated σ_2 stress contours (units of MPa) in glass/sapphire/polycarbonate *(g/s/p)* trilayers, d_g = 1000 μm and d_s = 500 μm, from contact with WC sphere, r_i = 3.18 mm at P = 430 N. **A,** With glass/sapphire adhesive (thickness 10 μm); **B,** without adhesive. Contact radius indicated at top surface.[57]

Once tested on suitable model monolith and bilayer structures (Fig. 8) (to evaluate the dimensionless coefficients), Equations 1 through 6 can be used to construct design diagrams for evaluating new dental material combinations (Fig. 10). Such diagrams can be invaluable in ranking prospective materials for maximum resistance to extraneous cracking in occlusal function. One of the future challenges of the materials community is to determine closed-form relations analogous to Equations 1 through 6 for trilayer structures, ultimately incorporating such relevant geometric features as specimen surface curvature (cuspal tooth radius). Until then, researchers will remain reliant on empiric, numeric (finite element) evaluations of individual case studies.

Five points related to clinical implications bear reiteration. (1) *Failure mode:* Radial cracks are believed to be largely responsible for the failure of clinical crowns. Cores in bilayer crowns may fracture before the veneers because of load transfer to the stiffer member in contact-induced flexure. Since these cracks remain confined to the subsurface core layers, at least in the first stages of their evolution, they may not be easily detectable. Metal cores are not subject to such brittle fracture (though they are subject to yield, which in turn can lead to fracture of the veneer), which may explain the relative success of porcelain-fused-to-metal crowns. More studies to determine the evolution of these cracks to failure, perhaps with stylized layer systems, appear to be warranted.

(2) *Materials:* From the standpoint of materials strengthening, the above results suggest that attention should focus more on the core than the veneer. Replacing the glass-infiltrated alumina currently used with a higher strength ceramic (Y-TZP zirconia, for example; Fig. 8) is one possibility currently being explored. Efforts to improve crown performance by seeking higher-strength porcelains might not be so effective (at least in all-ceramic crowns).

(3) *Flaw state:* Introduction of large flaws into the lower surfaces of ceramic crown layers can degrade strength (Fig. 11). Such flaws may arise from sand-

blasting by dental technicians to remove investment or surplus glass infiltrate at the inner crown surface (InCeram), from machining or shaping (CAD-CAM), or from diamond bur adjustments by the dentist in final seating. Avoidance of spurious flaws in preparation and handling of the core surfaces by minimizing potential damage procedures, or by etching such surfaces to remove some of the damage, could lead to improved crown lifetimes.

(4) *Layer thickness:* Clearly, it is essential to maximize crown thickness to reduce the chance of radial cracking. On the basis of the design diagrams presented here (Fig. 8), with due allowance for an additional degrading effect of surface preparation flaws (Fig. 11), a minimum occlusal reduction of 2 mm appears to be a conservative goal. Questions as to the most desirable ratio of veneer/core thickness in trilayers remain to be answered.

(5) *Cement:* Analysis of veneer/core interfaces with compliant intervening adhesive interlayers indicate that such interlayers can greatly enhance flexure, leading to radial cracking in the veneer. Ordinarily, this is not an issue with conventional processes used to fuse porcelains to the underlying cores. The presence of luting cement interlayers at the core/dentin interface might not be expected to be have quite such a strong effect on radial cracking, since the stiffnesses of cements generally do not differ much (typically < 50%) from that of the dentin. Nevertheless, the potential role of degraded dental cements, especially at the occlusal wall, is a contentious issue that remains to be properly understood.

Finally, there are other clinically relevant factors that need more study. Controlled contact experiments on the effect of cyclic loading in aqueous environments have been performed on ceramic monoliths (Fig. 4) but not on bilayers and trilayers. Water is expected to have access to the crown/dentin sublayer[8] through either the dentin or the luting cement. Studies in which sliding forces are superposed onto the normal Hertzian forces are known to profoundly decrease the critical loads for surface cone cracking,[58-60] with likely accompanying increases in wear, but analogous studies on subsurface radial cracking are only beginning. Preliminary findings in our laboratories indicate that the radial cracking is minimally affected by superposed sliding forces, suggesting that the conventional Hertzian approach is sufficient to characterize the most important damage mode. More complex load and cuspal geometry factors may be best handled by testing in mouth motion machines.

We would like to acknowledge important contributors to this work over the course of several years of research: E. D. Rekow, I. M. Peterson, Y.-G. Jung, Y.-W. Rhee, D. K. Kim, A. Pajares, P. Miranda, and H. Zhao. The following representatives from companies have maintained an active interest in our research program and have generously and unconditionally contributed materials for study: H. Hornberger, Vita Zahnfabrik; E. Levadnuk, Norton Desmarquest Fine Ceramics; and K. Chyung, Corning Inc.

REFERENCES

1. Lawn BR. Fracture of brittle solids. 2nd ed. Cambridge: Cambridge University Press; 1993.
2. Malament KA, Socransky SS. Survival of Dicor glass-ceramic dental restorations over 14 years: Part I. Survival of Dicor complete coverage restorations and effect of internal surface acid etching, tooth position, gender and age. J Prosthet Dent 1999;81:23-32.
3. Sjogren G, Lantto R, Tillberg A. Clinical evaluation of all-ceramic crowns (Dicor) in general practice. J Prosthet Dent 1999;81:277-84.
4. Fradeani M, Aquilano A. Clinical experience with Empress crowns. Int J Prosthodont 1997;10:241-7.
5. Sjogren G, Lantto R, Granberg A, Sundstrom BO, Tillberg A. Clinical examination of leucite-reinforced glass-ceramic crowns (Empress) in general practice: a retrospective study. Int J Prosthodont 1999;12:122-8.
6. Oden A, Andersson M, Krystek-Ondracek I, Magnusson D. Five-year clinical evaluation of Procera AllCeram crowns. J Prosthet Dent 1998;80:450-6.
7. McLaren EA, White SN. Survival of In-Ceram crowns in a private practice: a prospective clinical trial. J Prosthet Dent 2000;83:216-22.
8. Kelly JR. Clinically relevant approach to failure testing of all-ceramic restorations. J Prosthet Dent 1999;81:652-61.
9. DeLong R, Douglas WH. Development of an artificial oral environment for the testing of dental restoratives: bi-axial force and movement control. J Dent Res 1983;62:32-6.
10. Lawn BR. Indentation of ceramics with spheres: a century after Hertz. J Am Ceram Soc 1998;81:1977-94.
11. Lawn BR, Padture NP, Cai H, Guiberteau F. Making ceramics 'ductile.' Science 1994;263:1114-6.
12. Lawn BR, Lee KS, Chai H, Pajares A, Kim DK, Wuttiphan S, et al. Damage-resistant brittle coatings. Advanced Engineering Materials 2000;2:745-8.
13. Rhee YW, Kim HW, Deng Y, Lawn BR. Contact-induced damage in ceramic coatings on compliant substrates: fracture mechanics and design. J Am Ceram Soc 2001;18:1066-72.
14. Timoshenko S, Goodier JN. Theory of elasticity. 2nd ed. New York: McGraw-Hill; 1951. p. 372-7.
15. Guiberteau F, Padture NP, Lawn BR. Effect of grain size on Hertzian contact in alumina. J Am Ceram Soc 1994;77:1825-31.
16. Cai H, Stevens-Kalceff MA, Lawn BR. Deformation and fracture of mica-containing glass–ceramics in Hertzian contacts. J Mater Res 1994;9:762-70.
17. Frank FC, Lawn BR. On the theory of Hertzian fracture. Proc Royal Soc London 1967;A299:291-306.
18. Lawn BR, Wilshaw TR. Indentation fracture: principles and applications. J Mater Sci 1975;10:1049-81.
19. Guiberteau F, Padture NP, Cai H, Lawn BR. Indentation fatigue: a simple cyclic Hertzian test for measuring damage accumulation in polycrystalline ceramics. Philos Mag 1993;A 68:1003-16.
20. Hertz H. Hertz's miscellaneous papers. London: Macmillan; 1896. p. 146-83.
21. Chyung CK, Beall GH, Grossman DG. Microstructures and mechanical properties of mica glass-ceramics. In: Electron microscopy and structure of materials. Thomas G, Fulrath RM, Fisher RM, editors. Berkeley (CA): University of California Press; 1972. p. 1167-94.
22. Grossman DG. Structure and physical properties of Dicor/MGC glass-ceramic. In: Mörmann WH, editor. Proceedings of the international symposium on computer restorations. Chicago: Quintessence Publishing Co; 1991. p. 103-15.
23. Jung YG, Peterson IM, Kim DK, Lawn BR. Lifetime-limiting strength degradation from contact fatigue in dental ceramics. J Dent Res 2000;79:722-31.
24. Jung YG, Peterson IM, Pajares A, Lawn BR. Contact damage resistance and strength degradation of glass-infiltrated alumina and spinel ceramics. J Dent Res 1999;78:804-14.
25. Lawn BR, Lee SK, Peterson IM, Wuttiphan S. A model of strength degradation from Hertzian contact damage in tough ceramics. J Am Ceram Soc 1998;81:1509-20.
26. Kim DK, Jung YG, Peterson IM, Lawn BR. Cyclic fatigue of intrinsically brittle ceramics in contact with spheres. Acta Mater 1999;47:4711-25.

27. Yeo JG, Lee KS, Lawn BR. Role of microstructure in dynamic fatigue of glass-ceramics after contact with spheres. J Am Ceram Soc 2000;83:1545-7.
28. Lee KS, Jung YG, Peterson IM, Lawn BR, Kim DK, Lee SK. Model for cyclic fatigue of quasiplastic ceramics in contact with spheres. J Am Ceram Soc 2000;83:2255-62.
29. White SN, Zhao XY, ZhaokunY, Li ZC. Cyclic mechanical fatigue of a feldspathic dental porcelain. Int J Prosthodont 1995;8:413-20.
30. Rhee YW, Kim HW, Deng Y, Lawn BR. Brittle fracture versus quasiplasticity in ceramics: a simple predictive index. J Am Ceram Soc 2001;84:561-5.
31. Scherrer SS, de Rijk WG. The fracture resistance of all-ceramic crowns on supporting structures with different elastic moduli. Int J Prosthodont 1993;6:462-7.
32. Scherrer SS, de Rijk WG, Belser UC, Meyer JM. Effect of cement film thickness on the fracture resistance of a machinable glass-ceramic. Dent Mater 1994;10:172-7.
33. Tsai YL, Petsche PE, Anusavice KJ, Yang MC. Influence of glass-ceramic thickness on Hertzian and bulk fracture mechanisms. Int J Prosthodont 1998;11:27-32.
34. Kelly JR. Ceramics in restorative and prosthetic dentistry. Ann Rev Mater Sci 1997;27:443-68.
35. An L, Chan HM, Padture NP, Lawn BR. Damage-resistant alumina-based layer composites. J Mater Res 1996;11:204-10.
36. Wuttiphan S, Lawn BR, Padture NP. Crack suppression in strongly-bonded homogeneous/heterogeneous laminates: a study on glass/glass-ceramic bilayers. J Am Ceram Soc 1996;79:634-40.
37. Chan HM. Layered ceramics: processing and mechanical behavior. Ann Rev Mater Sci 1997;27:249-82.
38. Lee KS, Wuttiphan S, Hu XZ, Lee SK, Lawn BR. Contact-induced transverse fractures in brittle layers on soft substrates: a study on silicon nitride bilayers. J Am Ceram Soc 1998;81:571-80.
39. Jung YG, Wuttiphan S, Peterson IM, Lawn BR. Damage modes in dental layer structures. J Dent Res 1999;78:887-97.
40. Fischer-Cripps AC, Lawn BR, Pajares A, Wei L. Stress analysis of elastic–plastic contact damage in ceramic coatings on metal substrates. J Am Ceram Soc 1996;79:2619-25.
41. Wuttiphan S. Contact damage and fracture of ceramic layer structures. PhD thesis. College Park: University of Maryland; 1997.
42. Chai H, Lawn BR, Wuttiphan S. Fracture modes in brittle coatings with large interlayer modulus mismatch. J Mater Res 1999;14:3805-17.
43. Zhao H, Hu XZ, Bush MB, Lawn BR. Contact damage in porcelain/Pd-alloy bilayers. J Mater Res 2000;15:676-82.
44. Peterson IM, Pajares A, Lawn BR, Thompson VP, Rekow ED. Mechanical characterization of dental ceramics by Hertzian contacts. J Dent Res 1998;77:589-602.
45. Chai H, Lawn BR. Role of adhesive interlayer in transverse fracture of brittle layer structures. J Mater Res 2000;15:1017-24.
46. Hu XZ, Lawn BR. A simple indentation stress–strain relation for contacts with spheres on bilayer structures. Thin Solid Films 1998;322:225-32.
47. Kim HW, Deng Y, Miranda P, Pajares A, Kim DK, Kim HE, et al. Effect of flaw state on the strength of brittle coatings on soft substrates. J Am Ceram Soc 2001;84:2377-84.
48. Zhao H, Hu X, Bush MB, Lawn BR. Cracking of porcelain coatings bonded to metal substrates of different modulus and hardness. J Mater Res 2001;16:1471-8.
49. Xu HH, Smith DT, Jahanmir S, Romberg E, Kelley JR, Thompson VP, et al. Indentation damage and mechanical properties of human enamel and dentin. J Dent Res 1998;77:472-80.
50. Kinney JH, Balooch M, Marshall GW, Marshall SJ. A micromechanics model of the elastic properties of human dentine. Arch Oral Biol 1999;44:813-22.
51. Peterson IM, Wuttiphan S, Lawn BR, Chyung K. Role of microstructure on contact damage and strength degradation of micaceous glass-ceramics. Dent Mater 1998;14:80-9.
52. Langitan FB, Lawn BR. Hertzian fracture experiments on abraded glass surfaces as definitive evidence for an energy balance explanation of Auerbach's law. J Appl Phys 1969;40:4009-17.
53. Lawn BR, Evans AG, Marshall DB. Elastic/plastic indentation damage in ceramics: the median/radial crack system. J Am Ceram Soc 1980;63:574-81.
54. White SN, Caputo AA, Vidjak FM, Seghi RR. Moduli of rupture of layered dental ceramics. Dent Mater 1994;10:52-8.
55. Zeng K, Odén A, Rowcliffe D. Evaluation of mechanical properties of dental ceramic core materials in combination with porcelains. Int J Prosthodont 1998;11:183-9.
56. Wakabayashi N, Anusavice KJ. Crack initiation modes in bilayered alumina/porcelain disks as a function of core/veneer thickness ratio and supporting substrate stiffness. J Dent Res 2000;79:1398-404.
57. Miranda P, Pajares A, Guiberteau F, Cumbrera FL, Lawn BR. Contact fracture of brittle bilayer coatings on soft substrates. J Mater Res 2001;16:115-26.
58. Lawn BR. Partial cone crack formation in a brittle material loaded with a sliding indenter. Proc Royal Soc London 1967;A299:307-16.
59. Chiang SS, Evans AG. Influence of a tangential force on the fracture of two contacting elastic bodies. J Am Ceram Soc 1983;66:4-10.
60. Lawn BR, Wiederhorn SM, Roberts DE. Effect of sliding friction forces on the strength of brittle materials. J Mater Sci 1984;19:2561-9.

Reprint requests to:
DR BRIAN R. LAWN
MSEL: BUILDING 223, ROOM B309
NATIONAL INSTITUTE OF STANDARDS AND TECHNOLOGY
GAITHERSBURG, MD 20899
FAX: (301)975-5012
E-MAIL: brian.lawn@nist.gov

0022-3913/2001/$35.00 + 0. **10/1/119581**

doi:10.1067/mpr.2001.119581